Plant Ecology & Diversity

Productivity and carbon allocation in a tropical montane cloud forest in the Peruvian Andes

Cécile A.J. Girardin[a], Javier E. Silva Espejob[b], Christopher E. Doughty[c], Walter Huaraca Huasco[b], Dan B. Metcalfe[d], Liliana Durand-Baca[b], Toby R. Marthews[a], Luiz E.O.C. Aragao[e], William Farfán-Rios[f], Karina García-Cabrera[f], Katherine Halladay[a], Joshua B. Fisher[g], Darcy F. Galiano-Cabrera[b], Lidia P. Huaraca-Quispe[b], Ivonne Alzamora-Taype[b], Luzmila Eguiluz-Mora[b], Norma Salinas-Revilla[a], Miles R. Silman[f], Patrick Meir[h] & Yadvinder Malhi[i]

[a] Oxford University Centre for the Environment, Oxford University, Oxford, UK

[b] Herbario Vargas, Universidad Nacional San Antonio de Abad, Cusco, Peru

[c] Environmental Change Institute, University of Oxford, Oxford, UK

[d] Swedish University of Agricultural Sciences, Umeå, Sweden

[e] College of Life and Environmental Sciences, University of Exeter, Exeter, UK

[f] Biology, Wake Forest University, Winston-Salem, USA

[g] Jet Propulsion Laboratory, NASA, Pasadena, USA

[h] School of Geosciences, University of Edinburgh, Edinburgh, UK

[i] School of Geography and the Environment, University of Oxford, Oxford, UK
Published online: 17 Sep 2013.

PLEASE SCROLL DOWN FOR ARTICLE

Taylor & Francis
Taylor & Francis Group

Productivity and carbon allocation in a tropical montane cloud forest in the Peruvian Andes

Cécile A.J. Girardin[a]*, Javier E. Silva Espejo[b], Christopher E. Doughty[c], Walter Huaraca Huasco[b], Dan B. Metcalfe[d], Liliana Durand-Baca[b], Toby R. Marthews[a], Luiz E.O.C. Aragao[e], William Farfán-Rios[f], Karina García-Cabrera[f], Katherine Halladay[a], Joshua B. Fisher[g], Darcy F. Galiano-Cabrera[b], Lidia P. Huaraca-Quispe[b], Ivonne Alzamora-Taype[b], Luzmila Eguiluz-Mora[b], Norma Salinas-Revilla[a], Miles R. Silman[f], Patrick Meir[h] and Yadvinder Malhi[i]*

[a]*Oxford University Centre for the Environment, Oxford University, Oxford, UK;* [b]*Herbario Vargas, Universidad Nacional San Antonio de Abad, Cusco, Peru;* [c]*Environmental Change Institute, University of Oxford, Oxford, UK;* [d]*Swedish University of Agricultural Sciences, Umeå, Sweden;* [e]*College of Life and Environmental Sciences, University of Exeter, Exeter, UK;* [f]*Biology, Wake Forest University, Winston-Salem, USA;* [g]*Jet Propulsion Laboratory, NASA, Pasadena, USA;* [h]*School of Geosciences, University of Edinburgh, Edinburgh, UK;* [i]*School of Geography and the Environment, University of Oxford, Oxford, UK*

Background: The slopes of the eastern Andes harbour some of the highest biodiversity on Earth and a high proportion of endemic species. However, there have been only a few and limited descriptions of carbon budgets in tropical montane forest regions.
Aims: We present the first comprehensive data on the production, allocation and cycling of carbon for two high elevation (ca. 3000 m) tropical montane cloud forest plots in the Kosñipata Valley, Peruvian Andes.
Methods: We measured the main components and seasonal variation of net primary productivity (*NPP*), autotrophic (R_a) and heterotrophic (R_h) respiration to estimate gross primary productivity (*GPP*) and carbon use efficiency (*CUE*) in two 1-ha plots.
Results: *NPP* for the two plots was estimated to be 7.05 ± 0.39 and 8.04 ± 0.47 Mg C ha^{-1} year^{-1}, *GPP* to be 22.33 ± 2.23 and 26.82 ± 2.97 Mg C ha^{-1} year^{-1} and *CUE* was 0.32 ± 0.04 and 0.30 ± 0.04.
Conclusions: We found strong seasonality in *NPP* and moderate seasonality of R_a, suggesting that forest *NPP* is driven by changes in photosynthesis and highlighting the importance of variation in solar radiation. Our findings imply that trees invest more in biomass production in the cooler season with lower solar radiation and more in maintenance during the warmer and high solar radiation period.

Keywords: Andes; ecophysiology; net primary productivity; carbon use efficiency; respiration; elevation gradient; tropical montane forest; solar radiation

Introduction

The slopes of the eastern Andes harbour the most dynamic and ecologically diverse ecosystems in South America, with some of the highest biodiversity on Earth and a high proportion of endemic species (Young 1992; Gentry et al. 1993; Still et al. 1999; Killeen et al. 2007). Tropical montane cloud forests (TMCF) in particular are amongst the most fascinating yet poorly studied terrestrial ecosystems (Churchill 1993; Kapelle and Brown 2001). In addition, these dynamic and ecologically diverse ecosystems are adapted to strong environmental gradients over short distances (Pounds et al. 1999; Still et al. 1999; Myers et al. 2000; Bubb et al. 2004; Killeen et al. 2007). TMCFs are potential refuges for lowland plant species that may need to migrate in response to rapid climate change (Colwell et al. 2008; Feeley et al. 2010). As a result, the effects of changes in temperature, rainfall and cloud cover seasonality on tropical cloud forests are potentially very important, but remain poorly understood. As they combine low mean annual temperatures (characteristic of temperate forests) with small temperature seasonality (characteristic of tropical forests) and no dormant season (Körner 2012), understanding the carbon cycling of these unusual forest ecosystems could yield fundamental insights into the processes controlling their structure and function.

There has been a recent effort to improve our understanding of the carbon cycle of Amazonian forests, particularly through the RAINFOR forest inventory network (Malhi et al. 2002; Phillips et al. 2009). Much of this focus has been on individual components of productivity (Chambers et al. 2001; Clark et al. 2001), such as above-ground biomass in the RAINFOR project (Amazon Forest Inventory Network: Phillips et al. 2009; Malhi et al. 2006), above-ground woody production (Malhi et al. 2004) and litterfall (Chave et al. 2010). However, beyond biomass and biomass change, there has been much less attention paid to equally important aspects of the carbon cycle, such as net primary productivity (*NPP*), autotrophic respiration, gross primary production (*GPP*) and carbon use efficiency (*CUE*) (Malhi 2012). *GPP*, the rate of carbon fixation by

---

*Corresponding authors. Email: cecile.girardin@ouce.ox.ac.uk; yadvinder.malhi@ouce.ox.ac.uk

the ecosystem through photosynthesis, has been measured in the lowland tropical forests by using the eddy covariance method (e.g. Malhi et al. 1998; Araújo et al. 2004; Miller et al. 2004; Luyssaert et al. 2007). Comparison with flux tower studies (e.g. Malhi et al. 2009) has shown excellent agreement between measuring all the major components of *NPP* and autotrophic respiration, and carbon flux data from flux towers, greatly increasing confidence in the results of both methods. *NPP*, the net rate of construction of organic compounds by plants, is typically measured in the field by measuring or estimating the rate of production of new tissue in wood, leaves and fine roots (Clark et al. 2001). Total autotrophic respiration, the rate of efflux of CO_2 resulting from plant metabolic processes, can be measured by estimating and summing total leaf, stem and root rates of respiration (Heinemeyer et al. 2007). *CUE* is the ratio of *NPP* to *GPP*, or the fraction of carbon fixed that is allocated to biomass production. There is evidence that *CUE* might decrease with ongoing stress (Metcalfe et al. 2010), or increase after a disturbance event (DeLucia et al. 2007; Malhi et al 2009). This could have important implications for understanding long-term CO_2 emissions from rainforest ecosystems, but thus far is poorly represented in climate models predicting the fate of the Amazon in a warmer world.

Previous work on carbon budgets of tropical forests has largely focused on lowland forests. However, tropical montane systems could potentially yield valuable insights into how abiotic parameters control ecosystem processes (Malhi et al. 2010), one of the most important uncertainties in predicting the effects of future environmental change. In addition, the causes of the low productivity of tropical montane forests have long been a source of debate, with hypotheses focusing on temperature limitation of nutrient supply and physiology (Vitousek et al. 1986; Tanner et al. 1998), low light levels (Grubb et al. 1977; Metcalfe and Grubb 1997), humidity limitation of nutrient uptake (Bruijnzeel et al. 1993) and anaerobic conditions in waterlogged soils (Bruijnzeel and Veneklaas 1998). However, evidence of low productivity has tended to be based on low standing biomass or low woody growth rates, rather than measurements of above- and below-ground productivity.

Although there are a growing number of studies that have presented estimates of *NPP*, *GPP* and C allocation in tropical forest systems, TMCF remains underrepresented in the literature. As a result, any generalisation on the seasonal trends of climate and their close linkages with the seasonal cycle of *NPP* components in TMCFs remain tentative (Raich et al. 1997; Waide et al. 1998; Tanner et al. 1999; Herbert et al. 1999; Schuur and Matson 2001; Kitayama and Aiba 2002; Röderstein et al. 2005; Moser et al. 2008; Graefe et al. 2008). Considerable uncertainties remain regarding the fate of carbon sequestered in TMCF over short and long timescales. Hence, comprehensive assessments of ecosystem *NPP*, *GPP* and *CUE* over an annual cycle in plots located in close proximity with different microclimates, such as the one provided in this study, are required to provide a complete understanding of

the functioning of TMCFs and provide insights on how they might react to the predicted changes in climatic patterns.

This paper presents the first comprehensive carbon budgets from TMCF, comparing data from two 1-ha high elevation plots in the Peruvian Andes. We present annual and seasonal trends of *NPP* components, *GPP* and *CUE* averaged over a three-year period. We dissect the seasonality of carbon cycling and explore the close linkages between seasonal trends in productivity and climate variables as a means of understanding the ultimate controls of climate variables on the carbon budget. This study addressed the following specific questions: (1) how do the components of *NPP* and autotrophic respiration of these high-elevation tropical montane cloud forests vary over the seasonal cycle, and what are the main climatic drivers of productivity? (2) What are the seasonal trends of *GPP* and *CUE*? (3) How does the carbon budget (defined through *NPP*, R_a, *GPP* and *CUE*) compare between two cloud forest plots in close proximity, with different microclimates?

Materials and methods

Site history

Since 2003, the Andes Biodiversity Ecosystems Research Group (ABERG, http://www.andesconservation.org) has operated a number of permanent 1-ha plots in the Kosñipata Valley (Malhi et al. 2010): eight along the Trocha Union ridge-top trail (1855–3500 m a.s.l.), two at the Estación Biologica de Wayqecha (2825–3025 m a.s.l.) and two at San Pedro (1500–1750 m a.s.l.) where the valley enters the Madre de Dios region of Peru. Henceforth, we refer to these plots as the Kosñipata elevation transect. Partial data from the first Wayqecha plot have been reported in previous papers: soil carbon stocks in Zimmermann et al. (2009, 2010), forest above-ground productivity in Girardin et al. (2010), leaf physiology in van de Weg et al. (2012), modelling studies in Marthews et al. (2012a), stem respiration in Robertson et al. (2010) and the seasonality of below-ground productivity in Girardin et al. (2013). Here we provide the first comprehensive description (and seasonal cycle) of the carbon cycling from Wayqecha and the first data from Esperanza.

Site characteristics

The Esperanza (ESP, RAINFOR plot code ESP-01: 13° 11′ 25.1″ S, 71° 35′″ 49.2″ W, elevation 2825 m) and Wayqecha (WAY, RAINFOR plot code WAY-01: 13° 11′ 25.45″ S, 71° 35′ 13.56″ W, elevation 3025 m) plots are located in the cultural buffer zone of the Parque Nacional del Manú, Cusco, Peru (Table 1). Both plots are situated near the upper limit of the cloud forest zone, with the treeline at about 3200–3500 m elevation, where the forest makes a sharp transition to fire-dominated *puna* vegetation. The Wayqecha plot is only 100 m below the local treeline, and in an area where fires occasionally spread from the puna (although there was no obvious evidence of fire within the plot). The Esperanza plot is in a more humid location (data

Table 1.   Characteristics of the Esperanza and Wayqecha plots in the Kosñipata National Park, Cusco, Peru.

Site name	Esperanza	Wayqecha
Side code	ESP	WAY
Latitude (°)	−13.1903	−13.1904
Longitude (°)	−71.597	−71.5871
Elevation (m)	2825	3025
Mean annual air temperature (°C)	13.1	11.8
Annual precipitation (mm year^{-1})	1560	1560
Solar radiation (GJ m^{-2} year^{-1})	Not measured	3.51
Mean climatological water deficit (mm)	−394	−394
Aspect	West	East
Soil organic layer depth (cm)	32	32
Geology	Paleozoic slates and shales	Paleozoic slates and shales
Soil order	Umbrisol	Umbrisol
Soil C stock to 67 cm depth (Mg C ha^{-1})	277	614

Organic layer depth derived from Zimmermann (2009), soil carbon stock derived from A. Quesada (pers. comm.).

not shown), in a small local valley that is a focus of cloud convergence and formation, and has a forest composition more characteristic of tropical montane cloud forests (e.g. high incidence of tree ferns).

The soils in both plots are umbrisols (Table 1), ca. 67 cm deep, with an organic layer of ca. 30 cm (Table 1). The soils overlay Palaeozoic shale bedrock. The soils are highly acidic (pH 3.6; Zimmermann et al. 2009). The vegetation is closed-canopy forest with a relatively low mean canopy height (estimated as height of trees with diameter at breast height (dbh) >40 cm, 18 ± 5 m for ESP, and 20 ± 5 m for WAY) and moderately high plant species diversity of trees >10 cm dbh (56 species in ESP and 54 species in WAY). Mean wood density was estimated at 0.56 g cm^{-3} (ESP) and 0.58 g cm^{-3} (WAY). There were no differences between soil types, chemistry or physical characteristics, although we report significantly higher soil water content in ESP during the wet season.

Meteorological data

Solar radiation, air temperature, humidity and precipitation time series were collected from an automatic weather station (AWS) installed in a large clearing ca. 1 km from the WAY plot. The original data were measured with a resolution of at least 30 min for the period July 2005 to December 2010. These data were quality controlled to remove outliers. For temperature, values greater than 4 standard deviations from the mean were discarded, as were relative humidity (RH) values >100% and precipitation values >100 mm in 30 min. In the generation of a monthly time series for each variable, at least 90% of the maximum possible values in a given month were required to be present for that month to be included in the time series. The monthly time series were then gap-filled. For solar radiation, the monthly mean value for each missing month was used to gap-fill. For temperature, daily values from a nearby Senamhi (Peruvian Meteorological Service) station at Acjanaco (13.20° S, 71.62° W) were regressed against daily values from the AWS to correct for the difference between these two stations. The monthly

temperature time series was then gap-filled with corrected values from the Senamhi station. Relative humidity was calculated from wet and dry bulb temperatures, also from Acjanaco and measured at 07:00 h, 13:00 h and 19:00 h (local time), which were not adjusted. Any temperature or relative humidity values that were still missing after gap-filling with Senamhi data were filled using monthly means from the partially-filled time series. The precipitation time series was gap-filled by using values from the Senamhi station at Acjanaco at 07:00 h and 19:00 h (local time), which were aggregated to produce monthly estimates. If fewer than the maximum possible number of daily values were available, the monthly value was considered to be missing. Where these data were missing, monthly values from the nearest grid point of the Tropical Rainfall Measuring Mission (TRMM) (NASA Earth Observatory, Washington, DC, USA) 3B43 product were used. Maximum climatological water deficit (MCWD) was calculated by using the gap-filled monthly time series for precipitation according to the equations listed in Aragão et al. (2007).

Carbon fluxes

Measurements of *NPP*, R_a and R_h respiration were made in 2007 (WAY), and in 2009 (ESP and WAY) (Tables 2 and 3). The protocols used to estimate ecosystem C flux components were largely based on those developed by the RAINFOR-Global Ecosystem Monitoring (GEM) network. A detailed description is available online for download (http://gem.tropicalforests.ox.ac.uk) and in the online supplementary material accompanying this paper. Summaries of the different components quantified and the field methods and data processing techniques used are presented in Tables 2 and 3, respectively.

Net primary productivity (NPP)

All major *NPP* components were measured for this study in each of 25 subplots in each plot. We calculated above- and below-ground *NPP*, *NPP*$_{AG}$ and *NPP*$_{BG}$, respectively, using the following equations

Table 2.   Methods for intensive monitoring of carbon dynamics from Esperanza and Wayqecha plots in the Kosñipata National Park, Cusco, Peru (see also online supplemental material and RAINFOR-GEM manual (Marthews et al. 2012b)).

	Component	Description	Sampling period	Sampling interval
Above-ground net primary productivity (NPP_{AG})	Above-ground coarse wood net primary productivity (NPP_{ACW})	Annual forest inventory: all trees ≥10 cm dbh censused to determine growth rate of existing surviving trees and rate of recruitment of new trees. Stem biomass calculated using the Chave et al. (2005) allometric equation for tropical wet forests, employing diameter, height and wood density data. Four 15 × 15 m and one 20 × 20 m subplots established to census small trees (2.5–10 cm dbh)	2009–2011 (ESP) 2007–2011 (WAY)	Every year (trees ≥10 cm dbh) Every six months (trees 2.5–10 cm dbh)
		Seasonal growth: dendrometers installed on all trees (≥10 cm dbh) in each plot to determine the spatial-temporal and seasonal variation in growth.	2009–2011 (ESP) 2007–2011 (WAY)	Every three months
	Branch turnover net primary productivity ($NPP_{branch\ turnover}$)	Branches >2 cm diameter (excluding those fallen from dead trees) were surveyed within four 1 × 100 m transects; small branches were cut to include only the transect-crossing component, removed and weighed. Larger branches had their dimensions taken (diameter at three points) and all were assigned a wood density value according to their decomposition class (Harmon et al. 1995).	2009–2011	Every three months
	Litterfall net primary productivity ($NPP_{litterfall}$)	Litterfall production of dead organic material <2 cm diameter was estimated by collecting litterfall in 0.25 m² (50 × 50 cm) litter traps placed at 1 m above the ground at the centre of each of the 25 subplots (4 × 4 m) in each plot.	2007–2009	Every 14 days
	Leaf area index (LAI)	Canopy images recorded with a digital camera and hemispherical lens near the centre of each of the 25 subplots, at a standard height of 1 m, and during overcast conditions. LAI estimated from these images using CAN-EYE free software (https://www4.paca.inra.fr/can-eye).	2009–2010	Every month
	Loss to leaf herbivory ($NPP_{herbivory}$)	Leaves collected in the 25 litterfall traps in each plot were photographed prior to being dried. Leaf area was determined with ImageJ image analysis software (W. Rasband, Maryland, USA) to calculate the area of each individual leaf including the damage incurred by herbivory.	2008	Every two months
Below-ground net primary productivity (NPP_{BG})	Coarse root net primary productivity ($NPP_{coarse\ roots}$)	Not measured directly; estimated as 0.21 ± 0.03 of above-ground woody productivity, based on Jackson et al. (1996); Cairns et al. (1997).	n/a	Not directly measured
	Fine root net primary productivity ($NPP_{fine\ roots}$)	Sixteen ingrowth cores (mesh cages 12 cm diameter, to 30 cm depth) were installed in each plot. Cores were extracted and roots were manually removed from the soil samples in four 10 min time steps and the pattern of cumulative extraction over time was used to predict root extraction beyond 40 min. Root-free soil was then re-inserted into the ingrowth core. Collected roots were thoroughly rinsed, oven-dried at 80 °C to constant mass, and weighed. This process was repeated for each measurement thereafter.	2009–2011 (ESP) 2007–2011 (WAY)	Every three months

Table 2.   (*Continued*)

	Component	Description	Sampling period	Sampling interval
Autotrophic and hetertrophic respiration (R_a and R_h)	Total soil CO_2 efflux (R_{soil})	Total soil CO_2 efflux was measured using a closed dynamic chamber method with an infra-red gas analyzer and soil respiration chamber (EGM-4 IRGA and SRC-1 chamber, PP Systems, Hitchin, UK) sealed to a permanent collar in the soil. Soil surface temperature was measured with a T260 probe (Testo Ltd, Hampshire, UK) and soil moisture was recorded with a Hydrosense probe (Campbell Scientific Ltd, Loughborough, UK).	2009–2011 (ESP) 2007–2011 (WAY)	Every month
	Soil CO_2 efflux partitioned into autotrophic ($R_{rhizosphere}$) and heterotrophic ($R_{soilhet}$) components	We installed soil respiration partitioning experiments at each corner of the plot. In each corner, we installed three short collar tubes (10 cm depth) to measure total soil respiration and three long collar tube (40 cm depth) to exclude root and mycorrhizae respiration (R_a) Each of the three tubes were allocated different litter layer treatments (normal litter, no litter, double litter). A control experiment was carried out at the centre of each plot in order to assess the effects of root severing and soil structure disturbance that occurs during installation.	Feb 2009–Jun 2011	Every month
	Canopy respiration (R_{leaves})	In each plot, leaf dark respiration and photosynthesis at PAR levels of 1000 μmol m^{-2} s^{-1} were recorded for 15–25 trees with an IRGA and specialised cuvette (CIRAS 2 IRGA with PLC6 leaf cuvette, PP Systems, Hitchen, UK). For each tree, we randomly selected one branch, each from sunlit and shaded portions of the canopy and immediately re-cut the branches underwater to restore hydraulic connectivity (Reich et al. 1998).	Nov 2010 and Jul 2011	Once in dry season, once in wet season
	Above-ground live wood respiration (R_{stems})	Bole respiration was measured using a closed dynamic chamber method, from 25 trees distributed evenly throughout each plot at 1.3 m height with an IRGA (EGM-4) and soil respiration chamber (SRC-1) connected to a permanent collar, sealed to the tree bole surface.	Mar 2009–Dec 2010	Every month
	Coarse root respiration ($R_{coarse\ roots}$)	This component of respiration was not measured directly.	n/a	Not directly measured

$$NPP_{AG} = NPP_{ACW} + NPP_{litter\ fall} + NPP_{branch\ turnover}$$
$$+ NPP_{herbivory} \qquad (1)$$

$$NPP_{BG} = NPP_{fine\ roots} + NPP_{coarse\ roots} \qquad (2)$$

This neglects several small *NPP* terms, such *NPP* lost as volatile organic emissions, litter decomposed in the canopy or dropped from ground flora below the litter traps. Total R_a is estimated as

$$R_a = R_{leaves} + R_{stems} + R_{rhizosphere} \qquad (3)$$

Here we count root exudates and transfer to mycorrhizae as a portion of $R_{rhizosphere}$ rather than as *NPP*. In quasi-steady-state conditions (and on annual timescales or longer where there is no net change in plant non-structural carbohydrate storage), *GPP* should be approximately equal to plant carbon expenditure (*PCE*). Hence, we estimated *GPP* on the control plot as

$$GPP = NPP_{AG} + NPP_{BG} + R_a \qquad (4)$$

Table 3.   Data analysis techniques for intensive monitoring of carbon dynamics from Esperanza and Wayqecha plots in the Kosñipata National Park, Cusco, Peru (see also supplemental material and RAINFOR-GEM manual (Marthews et al. 2012b)).

	Component	Data processing details
Above-ground net primary productivity (NPP_{AG})	Above-ground coarse wood net primary productivity (NPP_{ACW})	Biomass calculated using the Chave et al. (2005) allometric equation for tropical moist forests: $AGB = 0.0776 \times (\rho\ dbh^2\ H)^{0.94}$, where AGB is above-ground biomass (kg), ρ is density of wood (g cm^{-3}), D is dbh (cm), and H is height (m). To convert biomass values into carbon, we assumed that dry stem biomass is 47.3% carbon (Martin and Thomas 2011). Where height data were not available, it was estimated by applying the Feldpausch et al. (2011) allometric equation.
	Branch turnover net primary productivity ($NPP_{branch\ turnover}$)	See RAINFOR-GEM manual (Marthews et al. 2012b, 61)) for description of decomposition status and surface area formulas.
	Litterfall net primary productivity ($NPP_{litterfall}$)	$NPP_{litterfall}$ was determined as: $NPP_{litterfall} = NPP_{canopy}-$ loss to leaf herbivory. Litterfall was separated into its components, oven-dried at 80 °C to constant mass and weighed. Litter was estimated to be 49.2% carbon, based on mean Amazonian values (S. Patiño, unpublished analysis).
	Leaf area index (LAI)	LAI estimated using true LAI output from the CAN-EYE software, which accounts for clumping of foliage, and assuming a fixed leaf inclination angle of 42.5°, based on mean estimates from ESP. Leaves were separated into sunlit and shaded fractions using the following equation: $F_{sunlit} = (1 - \exp(-K^*LAI))/K$ where K is the light extinction coefficient, and F_{sunlit} is the sunlit leaf fraction (Doughty and Goulden 2008). The model assumptions are randomly distributed leaves and $K = 0.5/\cos(Z)$, where Z is the solar zenith angle, which was set to 30° in this study.
	Loss to leaf herbivory ($NPP_{herbivory}$)	The fractional herbivory (H) for each leaf was calculated as: $H = (A_{nh} - A_h) / A_{nh}$, where A_h is the area of each individual leaf including the damage incurred by herbivory and A_{nh} is the leaf area prior to herbivory. The mean values of H were calculated across all leaves collected both per litterfall trap and per plot.
Below-ground net primary productivity (NPP_{BG})	Coarse root net primary productivity ($NPP_{coarse\ roots}$)	See RAINFOR-GEM manual (Marthews et al. 2012b, 47) for description and range of root:shoot ratio.
	Fine root net primary productivity ($NPP_{fine\ roots}$)	Roots were manually removed from the soil samples in four 10 min time steps, according to a method that corrects for underestimation of biomass of hard-to-extract roots (Metcalfe et al. 2007) and used to predict root extraction beyond 40 min (up to 100 min); we estimate that there was an additional 34% correction factor for fine roots not collected within 40 min. No correction was applied for fine root productivity below 30 cm.
Autotrophic (R_a) and hetertrophic (R_h) respiration	Total soil CO_2 efflux (R_{soil})	Soil surface temperature (T260 probe, Testo Ltd., Hampshire, UK) and moisture (Hydrosense probe, Campbell Scientific Ltd., Loughborough, UK) were recorded at each point after efflux measurement.
	Soil CO_2 efflux partitioned into autotrophic ($R_{rhizosphere}$) and heterotrophic ($R_{soilhet}$) components	The partitioning experiment allows estimation of the relative contributions of (1) surface organic litter, (2) roots, (3) mycorrhizae and (4) soil organic matter to total soil CO_2 efflux. Contributions are estimated from differences between collars subjected to different treatments, in excess of pre-existing spatial variation.
	Canopy respiration (R_{leaves})	To scale to whole-canopy respiration, mean dark respiration for shade and sunlit leaves were multiplied by the respective estimated fractions of total LAI. The wet season respiration mean was applied to all months with >100 mm rain; for the dry season months, measured dry season respiration was linearly scaled by the soil moisture saturation to allow for more continuous variation of leaf respiration. To account for daytime light inhibition of leaf dark respiration, we applied an inhibition factor: 67% of daytime leaf dark respiration, 34% of total leaf dark respiration (Malhi et al. 2009). These were calculated by applying the Atkin et al. (2000) equations for light inhibition of leaf respiration to a plot in Tapajós forest in Brazil (Malhi et al. 2009; Lloyd et al. 2010).
	Above-ground live wood respiration (R_{stems})	To estimate plot-level stem respiration, tree respiration per unit bole area was multiplied by bole surface area index (SAI) for each tree, estimated with the following equation (Chambers et al. 2004): $\log_{10}(SA) = -0.105 - 0.686 \log(dbh) + 2.208 \log(dbh)^2 - 0.627 \log(dbh)^3$, where dbh is bole diameter at 1.3 m height. Finally, for all 25 trees together we regressed mean annual bole respiration against total annual growth.
	Coarse root respiration ($R_{coarse\ roots}$)	Estimated by multiplying measured above-ground live wood respiration by 0.21.

Using these data, we estimated the *CUE* as the proportion of total *GPP/PCE* invested in total *NPP*

$$CUE = (NPP_{AG} + NPP_{BG})/(NPP_{AG} + NPP_{BG} + R_a)$$
$$(5)$$

Statistics and error analysis

Repeated-measures analysis of variance (ANOVA) was used to test for significant seasonal shifts in ecosystem carbon components between the plots. We estimated the relative seasonality index (SI = (maximum − minimum)/mean) for directly measured *NPP* (NPP_{ACW}, $NPP_{litterfall}$ and $NPP_{fine roots}$) and R_a (R_{stem}, R_{canopy} and $R_{fine roots}$) components. Unless stated otherwise, all estimated fluxes reported in this study are in Mg C ha^{-1} year^{-1}, and all reported errors show ±1 SE (errors are reported as ±SD for tree height). Conversions from µmol CO_2 m^{-2} s^{-1} to Mg C ha^{-1} year^{-1} were carried out as described in Marthews et al. (2012b, 75). Error propagation estimates were carried out for all combination quantities by using standard rules of quadrature (Hughes and Hase 2010), assuming that uncertainties were independent and normally distributed.

A key consideration is assignment and propagation of uncertainty in our measurements. There are two primary types of uncertainty. Firstly, there is sampling uncertainty associated with the spatial heterogeneity of the study plot and the limited number of samples. Examples include the variability among litter traps or among fine root ingrowth cores. Secondly, there is a systematic uncertainty associated with either unknown biases in measurement or uncertainties in scaling measurements to the plot level. Here we assume that most *NPP* terms were measured fairly precisely and sampled without large biases: hence, the *NPP* component measurements are dominated by sampling uncertainty, which can be reliably estimated assuming a normal distribution. On the other hand, some of the main autotrophic respiration terms are dominated by systematic uncertainty. This systematic uncertainty can be very hard to reliably quantify; here in each case we make an explicit and conservative estimate of the systematic uncertainty of key variables (Table 4).

Results

For conciseness, in the following text where values are given for the two plots separated by an oblique (/), the value are presented in the order Esperanza/Wayqecha.

Climate

The site showed evidence of strong seasonality in rainfall, ranging from over 300 mm month^{-1} in the peak rainy season (December to February) to less than 50 mm month^{-1} from May to September (Figure 1). Plot level soil moisture content (SWC) decreased significantly between May and September (dry season) 15.7%/15.7% and increased

Table 4. Annual mean canopy *NPP*, branch *NPP*, above-ground coarse wood *NPP*, coarse root *NPP*, fine root *NPP*, total above-ground *NPP*, total below-ground *NPP*, total *NPP*, canopy dark respiration, wood respiration, root respiration, coarse woody respiration, total autotrophic respiration, total heterotrophic respiration, total respiration, fraction of respiration above-ground and fraction below-ground *NPP*, *GPP* and *CUE* for 2 years of data for Esperanza and Wayqecha, Peru, 2009–2010.

	Esperanza			Wayqecha		
	Mean	Error	Total error	Mean	Error	Total error
$NPP_{litterfall}$*	2.69	0.28	0.28	3.67	0.28	0.28
NPP_{leaves}	1.96	0.23	0.23	2.52	0.18	0.18
$NPP_{flowers}$	0.05	0.03	0.03	0.10	0.01	0.01
NPP_{fruit}	0.21	0.03	0.03	0.22	0.03	0.03
NPP_{twigs}	0.42	0.12	0.12	0.67	0.13	0.13
$NPP_{herbivory}$	0.25	0.03	0.04	0.32	0.02	0.02
$NPP_{bromeliads}$	0.00	0.00	0.00	0.00	0.00	0.00
$NPP_{other epiphytes}$	0.07	0.02	0.02	0.13	0.02	0.02
$NPP_{branch turnover}$	0.75	0.07	0.07	0.54	0.05	0.05
$NPP_{ACW > 10cm}$	1.50	0.15	0.15	1.20	0.12	0.12
$NPP_{ACW < 10cm}$	0.15	0.02	0.02	0.15	0.02	0.02
$NPP_{coarse roots}$	0.32	0.03	0.03	0.25	0.03	0.03
$NPP_{fine roots}$	1.41	0.21	0.21	1.90	0.35	0.35
R_{leaves}	6.10	0.59	1.92	5.18	0.48	1.63
R_{stem}	4.87	0.49	1.54	7.69	0.74	2.42
$R_{fine roots}$	2.71	0.23	0.36	3.42	0.36	0.50
$R_{coarse roots}$	1.02	NA	0.52	1.61	NA	0.81
$R_{soilhet}$	6.81	0.54	0.87	7.22	0.73	1.02
R_a	14.71	0.81	2.54	17.90	0.97	3.07
R_{soil}	9.52	0.59	0.59	10.63	0.81	0.81
NPP_{total}	7.05	0.39	0.39	8.04	0.47	0.47
GPP	21.76	0.90	2.57	25.93	1.08	3.10
CUE	0.32	0.02	0.04	0.31	0.02	0.04

*$NPP_{litterfall}$ includes unidentified components, accounting for the discrepancy between total $NPP_{litterfall}$ and the sum of NPP canopy components. All data are given in Mg C ha^{-1} year^{-1}, unless otherwise stated. We report two primary types of uncertainty. Error is the sampling uncertainty associated with the spatial heterogeneity of the study plot and the limited number of samples. Total error also includes the systematic uncertainty associated with either unknown biases in measurement, or uncertainties in scaling measurements to the plot level.

to 33.7%/28.9% SWC during the rest of the year. The ESP plot had a significantly wetter wet season than the WAY plot. There was a distinct seasonality in solar radiation, with higher values in the late and early (August to November). The mean annual air temperature was ca. 12.5 °C and there was a mild seasonality in monthly means of air temperature, with a maximum of 11.5 °C during the peak of the wet season and a minimum of 10 °C in the driest months. There was little seasonality in relative humidity, though we observed a small dip in the peak dry season (Figure 1(c)). The mean annual rainfall over the period was ca. 1560 mm; this may be lower than the long-term mean because of a drought in 2010. There is also likely to be a small additional precipitation input through cloud interception, particularly in the dry season, but this has not been quantified for these plots. Soil moisture content (top 30 cm) was not significantly different ($P > 0.05$) between the plots, with only slightly higher values in ESP than WAY (24.7 ± 0.49%/23.7 ± 0.40% water). On average, the WAY plot at 3025 m a.s.l. was drier and received higher annual light
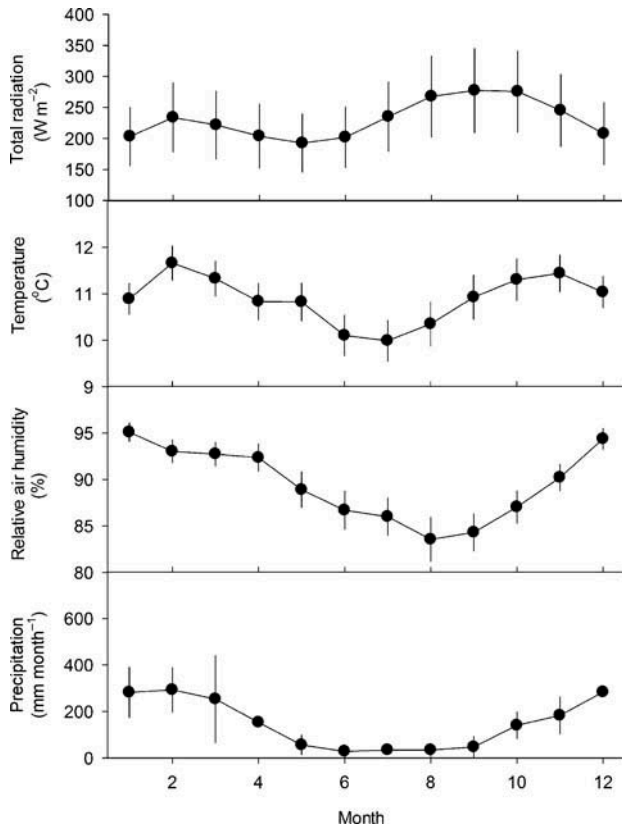
Figure 1. Climate data from a meteorological station located at 13.20° S, 71.62° W for (a) total radiation (W m^{-2}); (b) mean monthly temperature (°C); (c) atmospheric relative humidity (water vapour/saturated water vapour); (d) mean monthly precipitation (mm month^{-1}). Grey indicates data gap-filled with only monthly means as opposed to an alternative data source – 32% of values are missing. Error bars show ±1 SD.

incidence (not shown) than the ESP plot at 2825 m. The latter was situated on a ridge that acted as a trigger for cloud formation, resulting in a cloudier and wetter atmospheric environment than WAY, due to increased cloud immersion. Rapp et al. (forthcoming) reported that the diurnal rhythm of light availability did not vary from one season to the next, although light intensity was significantly higher during the wet season. Both sites are frequently immersed by clouds in the dry season.

The forests studied here experience an extended five-month-long dry season (May to September) and two solar radiation peaks, in March and September. At these high elevations, the lowest solar radiation incidence coincides with a period of low and frequent cloud immersion (dry season, April to July). This may be explained by the lower height of the cloud base, and frequent cloud immersion during the dry season, in turn, is explained by a capping thermal inversion led by trade winds running into the mountain (Foster 2001). Cloud base heights are frequently above the mountains during the wet season (December to February).

Biomass and net primary productivity

Seasonality of NPP *and* R$_a$. All above-ground components of net primary productivity displayed distinct
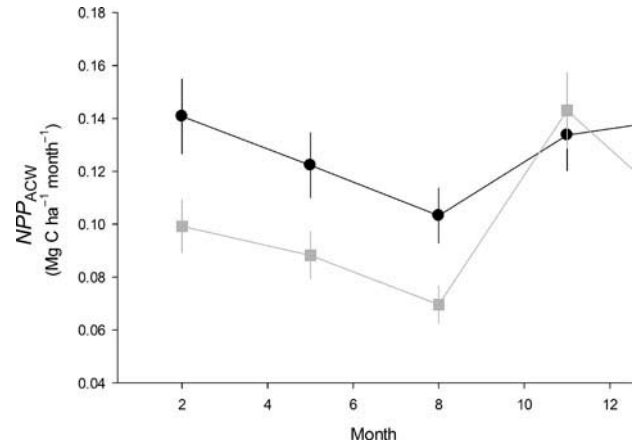

Figure 2. Above-ground woody *NPP* (Mg C ha^{-1}) determined by using dendrometer bands, measured every three months over a two-year period in Esperanza (black circles) and Wayqecha (grey squares), Peru. Error bars show ±1 SE assuming that each measurement on each tree is accurate to 1 mm.

seasonal patterns, with varying intensities (Figures 2 and 3). We found a strong seasonality of *NPP* (SI = 0.99/0.82) and minor seasonal variation in *R*$_a$ (SI = 0.50/0.43). The seasonal trend of each component is described in more detail below.

Above-ground woody biomass and NPP. Mean wood density was estimated at 0.56/0.58 g cm^{-3} and the mean (±SD) height of canopy trees (>40 cm dbh) was 18 ± 5 m/20 ± 5 m. Total above-ground biomass for trees >10 cm dbh was 59.5/72.9 Mg C ha^{-1}. Total plot-level biomass for small trees (<10 cm dbh) was 5.4/13.3 Mg C ha^{-1}. Hence, total plot-level above-ground biomass was lower in WAY (64.9 Mg C ha^{-1}) than in ESP (86.2 Mg C ha^{-1}). Mean above-ground coarse wood includes stem and branches (ACW) productivity for the years 2006, 2009, 2010 and 2011 was estimated at 1.50 ± 0.15/1.20 ± 0.12 Mg C ha^{-1} year^{-1} for stems >10 cm dbh, and at 0.15 ± 0.02, 0.15 ± 0.02 Mg C ha^{-1} year^{-1} for stems <10 cm dbh. Hence, total stand level productivity was higher in WAY than in ESP at 1.65 ± 0.15 vs. 1.35 ± 0.12 Mg C ha^{-1} year^{-1} (Table 2).

To estimate the effect of moisture expansion during the wet season on tree growth, we separated the live trees with almost no overall tree growth (*NPP*$_{ACW}$ < 0.05 kg C tree^{-1} year^{-1}, *n* = 30/38) and measured their seasonal trends. The mean seasonal amplitude of these slow-growing trees peaked at the height of the dry season (July) and was lowest at the start of the wet season (October). We estimated that plot-level moisture expansion between April and November was the equivalent of 0.016/0.02 Mg C ha^{-1} year^{-1}.

Canopy NPP. Mean annual fine litterfall was significantly (*P* < 0.001) lower in ESP (2.69 ± 0.28 Mg C ha^{-1} year^{-1}) than WAY (3.67 ± 0.28 Mg C ha^{-1} year^{-1}) (Table 2), a difference predominantly caused by the significantly (*P* < 0.001) lower leaf litter production in ESP (1.96 ± 0.23/2.52 ± 0.18 Mg C ha^{-1} year^{-1}). Total canopy *NPP*
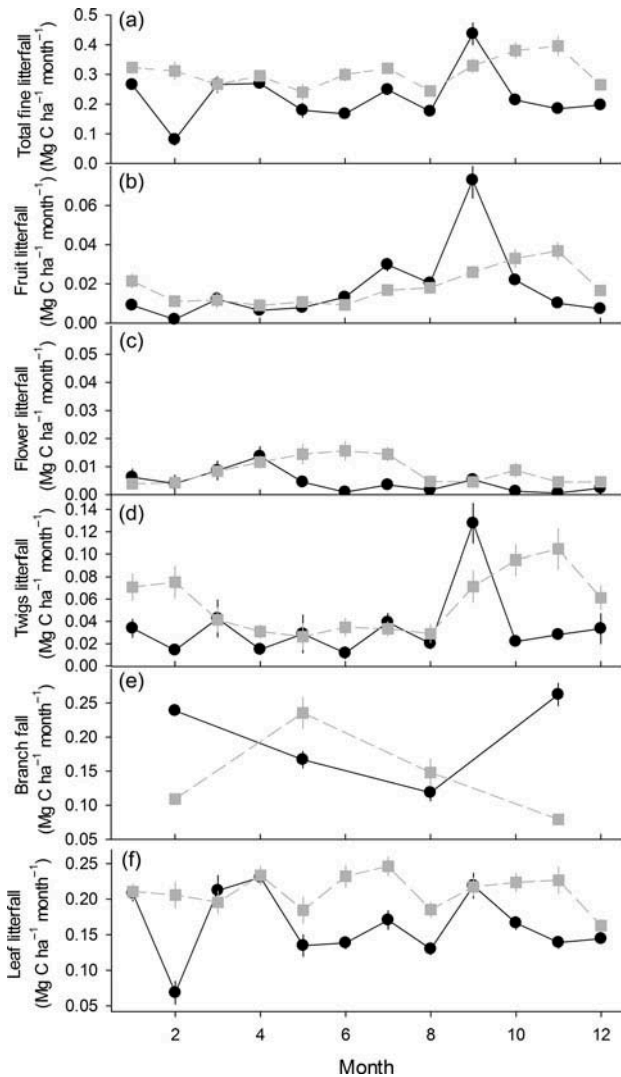
Figure 3. Sum of the monthly collections from 25 litterfall traps of (a) total fine litterfall; (b) fruit; (c) flowers; (d) twigs; (e) branches; (f) leaves in Esperanza (black circles) and Wayqecha (grey squares), Peru, 2009–2010. Error bars show ±1 SE.

(including $NPP_{\text{herbivory}}$) was 2.94 ± 0.23 Mg C ha^{-1} year^{-1} in ESP and 3.99 ± 0.18 Mg C ha^{-1} year^{-1} in WAY. In terms of litter fractions for ESP/WAY, the litterfall was composed of 73%/69% leaf fall, 2%/3% flower fall, 8%/6% fruit fall, 16%/18% twig fall, and the remaining fraction allocated to epiphytes and unidentifiable material, indicating a greater allocation to leaves and twigs in WAY. Based on the three-monthly transects, the mean total annual $NPP_{\text{branch turnover}}$ was $0.75 \pm 0.07/0.54 \pm 0.05$ Mg C ha^{-1} year^{-1}. In both plots, there was a lack in overall trend in $NPP_{\text{litterfall}}$ seasonality, although we recorded strong seasonal trends in all components but leaves, with a broad minimum over the dry season (May to September). Seasonality of litterfall production closely followed that of solar radiation incidence, albeit with a moderate seasonal amplitude. Leaf litterfall showed only moderate seasonality throughout the annual cycle, with a minimum over the dry season. In both plots, litterfall of flower, fruit, twigs, bromeliads and other epiphytes showed strong seasonal trends. Fruit,

twigs, bromeliads and other epiphytes in litterfall reached a minimum over the dry season and sharply increased at the end of the dry season (ESP) and start of the wet season (WAY), coinciding with the transition season at the end of the low-cloud immersion period and the peak in solar radiation levels (August to November). Flower litterfall also reached a maximum during a transition season, at the end of the wet season in ESP (February to April) and at the start of the dry season in WAY (May to July).

Fine root NPP. Based on the exponential decrease in separated fine root material per 10-min sampling period, we estimated that an additional 34%/34% of fine root *NPP* remained in each ingrowth core following our 40-min measuring interval. We assumed no root growth below our ingrowth cores as the soil is very close to bedrock (67 cm depth). $NPP_{\text{fine root}}$ was significantly higher ($P < 0.05$) in ESP (1.41 ± 0.21 Mg C ha^{-1} year^{-1}) than WAY (1.90 ± 0.35 Mg C ha^{-1} year^{-1}). Fine root growth showed a strong seasonal cycle, significantly higher ($P < 0.001$) in the dry season, with an increase of 53%/62 % from February to August (Figure 4).

Herbivory. We recorded a mean herbivory fraction of 12.5 ± 1.1 %/13.7 ± 0.9 % ($n = 25$) in ESP and WAY. Correcting the measured $NPP_{\text{litterfall}}$ in both plots according to this fraction, we estimated an *NPP* loss to leaf herbivory ($NPP_{\text{herbivory}}$) of $0.25 \pm 0.04/0.32 \pm 0.02$ Mg C ha^{-1} year^{-1}. This relatively large term emerges from a combination of a high herbivory fraction and high leaf production rates.

Leaf area index and leaf production. Mean leaf area index (LAI) was 4.51 ± 0.19 m^2 m^{-2} in ESP and 3.73 ± 0.14 m^2 m^{-2} in WAY. The LAI in ESP (not shown) was constant throughout the year, averaging 4.52 ± 0.20 m^2 m^{-2} in the dry season (June to October), and 4.50 ± 0.18 m^2 m^{-2} during the wet season. In WAY, LAI was more seasonal, with an increase in LAI during the dry season and a
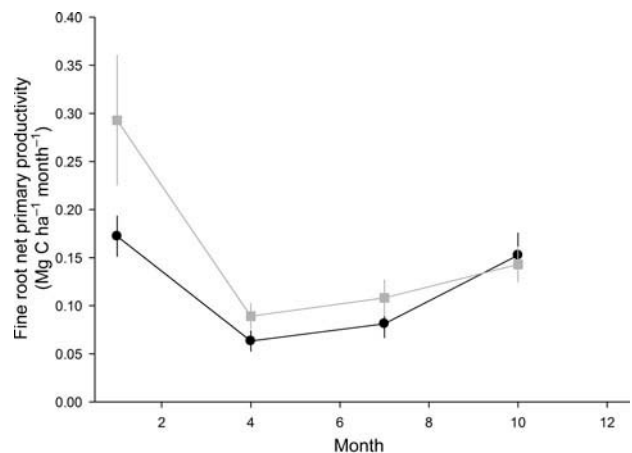

Figure 4. Fine roots *NPP* from 16 ingrowth cores collected every three months over a two-year period for Esperanza (black circles) and Wayqecha (grey squares), Peru, 2009–2010. Error bars show ±1 SE.

slight decrease over the wetter months, from 4.06 ± 0.15 to 3.23 ± 0.14 m^2 m^{-2}. Changes in LAI and leaf litterfall allowed us to estimate the seasonal cycle of leaf production. In both plots, leaf shedding (litterfall) began in May/June, matched by a decline in LAI. By August, LAI halted its decline despite a further steep rise in leaf fall rates, indicating that the production of new leaves was balancing the loss of old leaves. Overall, leaf production showed a mild peak in both plots in the late dry season (August to October), which also matched the peak in leaf fall rates, indicating higher rates of leaf shedding and replacement in this period.

Respiration

Soil respiration. To control for the effect of soil perturbation during the installation phase of our partitioning experiment, we investigated the effect of a disturbance on soil cores. Total respiration measurements (R_{total}) were not significantly different ($P > 0.05$) in ESP, averaging 1.33 ± 0.069 μmol m^{-2} s^{-1} for the undisturbed cores, and 1.44 ± 0.081 μmol m^{-2} s^{-1} for the disturbed cores, a 9% difference. In WAY, the undisturbed cores resulted in significantly lower ($P < 0.05$) values, averaging 2.22 ± 0.088 μmol m^{-2} s^{-1}, compared to the disturbed cores averaging 2.48 ± 0.089 μmol m^{-2} s^{-1}, a difference of 11%. There was no significant trend in this difference over inter-annual or seasonal timescales in either plot.

We calculated the mean percentage respiration attributable to the rhizosphere by subtracting monthly values of tubes excluding rhizosphere respiration from those including rhizosphere and heterotrophic respiration. Mean total rhizosphere respiration in ESP and WAY was $3.73 \pm 0.63/5.03 \pm 0.95$ Mg C ha^{-1} year^{-1}, with no significant difference. The fraction of carbon allocated to rhizosphere respiration was estimated at 28%/31% of soil respiration (monthly mean), decreasing significantly ($P < 0.001$) to 23%/30% during the dry season (June to October) compared to a mean of 31%/33% during the rest of the year (Figure 5).

Total soil respiration had a significant seasonal cycle ($P < 0.001$) and was lowest in the dry season (May to September) in both plots. Total mean annual soil respiration was not significantly different between sites, averaging $9.52 \pm 2.68/10.63 \pm 3.54$ Mg C ha^{-1} year^{-1}. Total heterotrophic soil respiration had a significant seasonal cycle ($P < 0.001$) and was lowest in the dry season. Total mean annual soil heterotrophic respiration was significantly lower ($P < 0.05$) in ESP, averaging 6.81 ± 0.87 Mg C ha^{-1} year^{-1}, than in WAY, averaging 7.22 ± 1.02 Mg C ha^{-1} year^{-1}.

Live woody biomass respiration. Total woody surface area of trees >10 cm dbh was estimated at 13,570/ 17,830 m^2 ha^{-1}. Total woody surface area of trees <10 cm dbh was estimated at 1048/2481 m^2 ha^{-1} (see equation in Table 3). This summed to a stem area index (SAI) of 1.46 for ESP and 2.03 for WAY. We measured stem respiration on 25 trees per plot. R_{stem} was significantly lower ($P <$
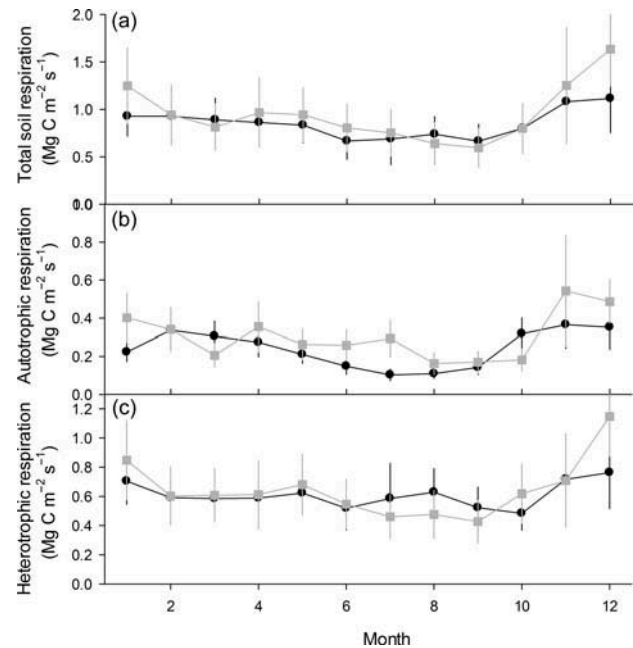

Figure 5.   (a) Total soil respiration from 25 collars measured monthly; (b) autotrophic soil respiration; (c) heterotrophic soil respiration from a two-year period in Esperanza (black circles) and Wayqecha (grey squares), Peru, 2009–2010. Autotrophic respiration was determined by an exclusion experiment ($n = 16$) where respiration was measured from tubes where roots and mycorrhizae were removed. Error bars show ± 1 SE.

0.05) in ESP than WAY, estimated at $1.09 \pm 0.12/1.24 \pm 0.14$ μmol m^{-2} s^{-1}.

To scale these measurements to the plot level we looked for a relationship between woody *NPP* and woody respiration for those 25 trees. There was a significant positive linear relationship between woody *NPP* and stem respiration for both ESP and WAY. We found that the trees measured for woody respiration grew faster than average and therefore had to reduce our estimates for respiratory fluxes by 7% in ESP and 14% in WAY when scaled to the entire plot.

We then multiplied total plot above-ground coarse woody surface area by our scaled woody respiration fluxes (Figure 6). There was a significant seasonal cycle ($P < 0.001$) in wood respiration in both sites, although it did not relate to precipitation, temperature or solar radiation seasonality. R_{stem} seasonality followed the trends of NPP_{ACW} seasonality in both plots (Figures 2 and 6). Total annual woody respiration in ESP was 4.87 ± 1.54 Mg C ha^{-1} year^{-1} and 7.69 ± 2.42 Mg C ha^{-1} year^{-1} for WAY.

Leaf respiration and photosynthesis. We measured dark leaf respiration and maximum photosynthetic capacity for sunlit and shaded leaves on trees evenly distributed throughout our plots. There was evidence of low seasonality in both plots, and no significant differences were found between plots. In both plots, shade and sun leaf respiration values were significantly higher in the wet season. However, when scaled up to the whole canopy, there
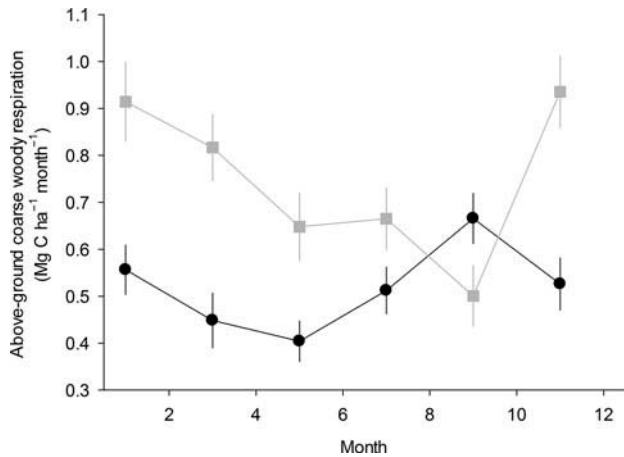
Figure 6. Above-ground wood respiration per unit forest area from collars on 25 trees measured every three months and multiplied by the total woody surface area of the plot in Esperanza (black circles) and Wayqecha (grey squares), Peru, 2009–2010. We scaled total respiration by woody *NPP* to account for different tree growth rates in the two plots. Error bars show ± 1 SE multiplied by woody surface area.

was little seasonality in our estimated canopy leaf respiration (Table 5). Total annual canopy respiration was estimated to be 6.10 ± 1.92 Mg C ha^{-1} year^{-1} in ESP and 5.18 ± 1.63 Mg C ha^{-1} year^{-1}. We did not find a significant relationship between NPP_{ACW} and dark leaf respiration. There was no difference in light-saturated sunlit leaf photosynthesis between plots or between seasons within each plot.

Annual NPP*, autotrophic respiration and* CUE. The measured and estimated components of *NPP* were summed, using Equations (1) and (2) to estimate a plot-level *NPP* of

Table 5. Leaf dark respiration values (μmol m^{-2} s^{-1}), by season and by leaf position (sun vs. shade) in Esperanza and Wayqecha, Peru, 2010.

	Dry season		Wet season	
	Sun leaves	Shade leaves	Sun leaves	Shade leaves
Esperanza	0.68 ± 0.05	0.57 ± 0.07	0.60 ± 0.05	0.48 ± 0.05
Wayqecha	0.57 ± 0.05	0.52 ± 0.04	0.58 ± 0.05	0.55 ± 0.06

Dry season is from May to September, wet season is from October to April. These respiration values are the values that the leaf would respire theoretically at the mean annual temperature of the site (12.5 °C).

7.05 ± 0.39 Mg C ha^{-1} year^{-1} for ESP and 8.04 ± 0.47 Mg C ha^{-1} year^{-1} for WAY. The three estimated components of autotrophic respiration were summed by using Equation (3) to estimate total autotrophic respiration at 14.71 ± 2.54 Mg C ha^{-1} year^{-1} for ESP and 17.90 ± 3.07 Mg C ha^{-1} year^{-1} for WAY. The sum of *NPP* and autotrophic respiration gave estimated values of *GPP* of 21.76 ± 2.57 Mg C ha^{-1} year^{-1} for ESP and 25.93 ± 3.10 Mg C ha^{-1} year^{-1} for WAY (Figure 7). The ratio of *NPP* to *GPP* is an ecosystem carbon use efficiency (*CUE*) of $0.32 \pm 0.04/0.31 \pm 0.04$. Both plots showed remarkable synchrony in total net primary productivity seasonality: above- and below-ground productivity remained low during the dry season, increasing at the end of the dry season and reaching a maximum at the end of the wet season (Figure 8).

Discussion

This paper presents the first complete time series of the main components of *NPP* and R_a over an annual seasonal cycle in a tropical montane cloud forest.

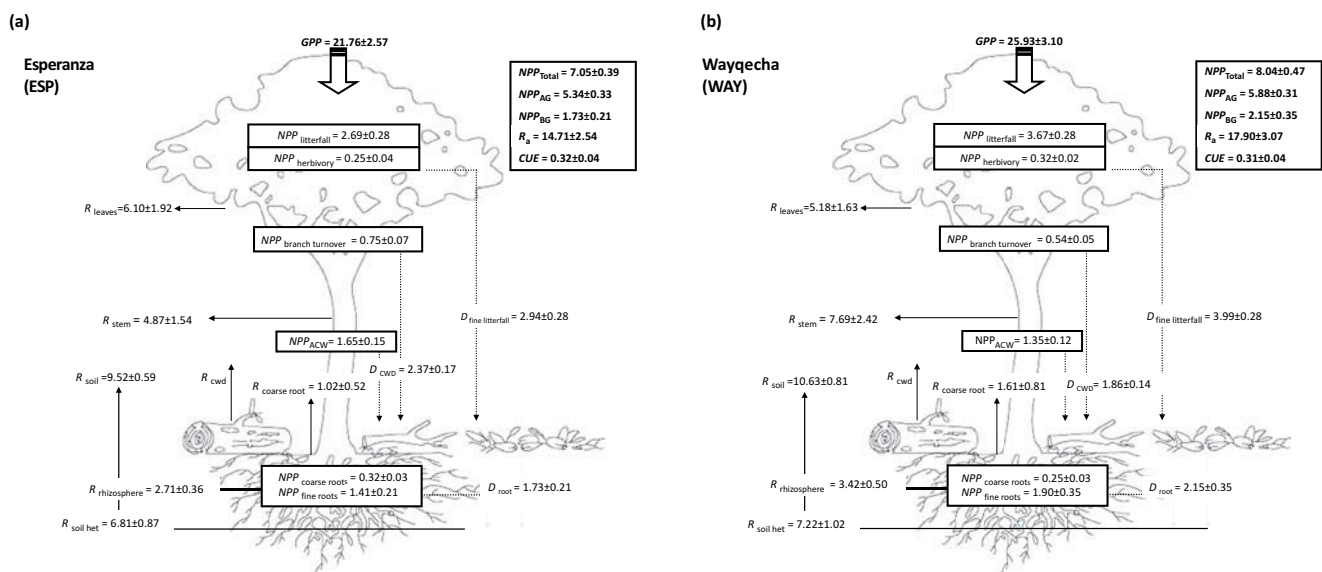Figure 7. Diagram showing annual means for all components of respiration, *NPP*, *GPP* and *CUE* for (a) Esperanza (2825 m); (b) Wayqecha (3025 m), Peru. *D* represents the decomposition of biomass: $D_{\text{fine litterfall}} = NPP_{\text{litterfall}}$, $D_{\text{CWD}} = (NPP_{\text{ACW}} + NPP_{\text{branch turnover}})$ and $D_{\text{root}} = (NPP_{\text{coarse roots}} + NPP_{\text{fine roots}})$.
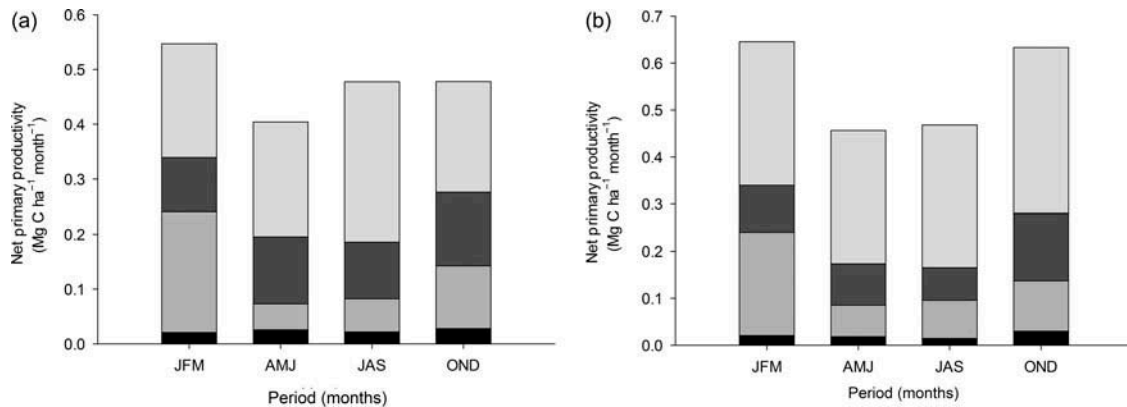
Figure 8.   Seasonal budget of net primary productivity of coarse roots (black), fine roots (mid grey), above-ground coarse wood (dark grey), and canopy (light grey) in (a) Esperanza; (b) Wayqecha, Peru, 2009–2010. Estimates are weighted means over three months (e.g. JFM, January, February and March).

Seasonality of NPP *and respiration components*

The seasonal values of *NPP* for above-ground coarse wood, canopy and fine root made up most of the *NPP* budget, but for completeness we also made assumptions about the seasonal variation of the remaining components. We assumed that $NPP_{branch\ turnover}$, $NPP_{ACW\ <\ 10\ cm}$, and $NPP_{coarse\ roots}$ followed the same seasonal cycle as $NPP_{ACW\ >\ 10\ cm}$, and used a multiplying factor of 1.25/1.15, based on the annual ratio of these terms in each plot (Table 4).The lower multiplying factor reported for WAY is attributed to a slower productivity of coarse roots, branch turnover and ACW > 10 cm dbh.

The present study found remarkably close linkages between the seasonal trends in climate variables and the seasonal budget of *NPP* and its components (Figures 1 and 7). Total *NPP* closely followed the seasonality of light and temperature, decreasing significantly during the cloudier and cooler dry season. In terms of relative allocation, we found a shift in allocation of *NPP* from above-ground coarse woody material to fine roots during the wet season, when solar radiation was at its highest. In both plots, more C was allocated to NPP_{ACW} at the start of the wet season, and $NPP_{fine\ roots}$ was prioritised at the expense of NPP_{ACW} by mid-wet season.

Whereas leaf litterfall, and hence total litterfall, only showed moderate seasonal amplitude (Figure 3), the phenology of flowering and fruiting provided insights on the linkages between forest reproduction and climatic variables. In ESP, the increase in flower productivity at the end of the wet season was remarkably closely linked to the peak in solar radiation. The subsequent peak in fruiting productivity at the start of the wet season also coincided with a peak in solar radiation. Nonetheless, the flowering and fruiting phenology in WAY was shifted forward by two months, suggesting that the seasonal trend was perhaps driven by phenological rhythms of dominant families rather than being directly driven by solar radiation. WAY was more diverse than ESP and included families

that had bigger flower clusters and possibly later flowering (Aquifoliaceae, Caprifoliaceae, Asteraceae). In particular, Asteraceae species show diversification in their flowering times and flowering midpoints within favourable periods (Torres and Galetto 2011).

The fruiting season peaks mainly during the wet season when there is enough moisture for germination (Zimmerman et al. 2007). As expected, flowering phenology was closely related to fruiting phenology, occurring two to four months before fruiting (van Schaik et al. 1993; Leigh 1999). The litterfall phenology observed in ESP was more characteristic of the Kosñipata montane forest, as described in Girardin et al. (2014). The strong decline in reproductive function (defined as production of flowers and fruit) over the cloud immersion period may be attributed to a decrease in light incidence (Marthews et al. 2012a) and an increase in the prevalence of pathogens (e.g. fungi) resulting from persistent humidity (Leigh 1999). Patterns of carbon allocation to canopy components change along the Kosñipata elevation transect, showing evidence of increased allocation to reproductive components during the wet season within the cloud immersion zone (Marthews et al. 2012a). A large seasonality in *NPP* and minor seasonal variation in R_a (as measured by seasonality index) suggest that forest *NPP* is driven mostly by changes in photosynthesis while R_a remains more or less constant, implying one should focus on 'light and dark seasons' rather than seasons defined by temperature (summer/winter) or water availability (wet/dry). Nonetheless, we continue to describe the annual cycle in terms of wet (i.e. light) and dry (i.e. light) seasons for clarity. In forests with a pronounced dry season, the phenology of reproductive organs appeared to vary according to moisture availability (Girardin et al. 2014), but the lack of moisture stress in our cloud forest plots (Zimmermann et al. 2009) meant that forest phenology were related predominantly to light availability, with increasing allocation to reproductive organs when light was in abundance (wet season).

We provide the first detailed description of the seasonal variation in the main components of autotrophic respiration from a TMCF (Figure 5). We observed a small seasonal amplitude in autotrophic respiration (R_a), with the seasonal patterns of R_a and R_h broadly following those of $NPP_{fine roots}$. Soil respiration seasonality was principally driven by R_h, concurring with findings by Heinemeyer et al. (2007) and Zimmermann (2009). We observed a strong seasonality in *NPP* and moderate seasonality in R_a. Although we lack information to accurately quantify the seasonal cycle of *CUE*, our findings imply that *CUE* is likely to show similar seasonality in both plots, with a lower *CUE* during the dry season. The seasonal trend of R_a further suggests that trees invest more in biomass productivity in the cooler and darker season and more in maintenance during the warmer and high solar radiation incidence period. Our findings are in agreement with the results reported by Robertson et al. (2010), who found a decline in growth to maintenance respiration along the Kosñipata elevation transect, and with the theory proposed by van Oijen et al. (2010), according to which a growth to maintenance respiration ratio close to zero occurs at the treeline and determines the limit of the treeline (Körner et al. 2012; Marthews et al. 2012a).

The carbon cycle of an upper montane cloud forest

Our approach to intensive carbon cycling measurements provides a complete overview of the carbon cycle: we provide a bottom-up estimate of *GPP* by summing the rate of carbon assimilated into biomass (*NPP*) and emitted through autotrophic respiration (R_a). Although these two plots are located within 1 km of each other, they differ significantly in terms of biomass, *NPP* and *GPP*. Stand biomass and total *NPP* were significantly higher in WAY (difference in NPP_{total} of 1.06 ± 2.43 Mg C ha^{-1} year^{-1}), this was principally driven by NPP_{canopy}. *GPP* was significantly higher in WAY than in ESP (a difference of 3.26 ± 3.50 Mg C ha^{-1} year^{-1}), this was driven by a higher R_a. The substantial differences in carbon cycling (most notably in *GPP*) between the two plots despite their similarities in climate and soil conditions may be explained by different stand ages and species composition. Tree height of trees >40 cm dbh and total above-ground biomass estimates were higher in WAY than ESP. Nonetheless, above-ground woody biomass estimates for both plots were within the range of estimates in Andean TCMF above 2500 m a.s.l. reported in the literature (66–146.95 Mg C ha^{-1} year^{-1}, Moser et al. 2006; Leuschner et al. 2007; Graefe et al. 2008; Moser et al. 2008; Girardin et al. 2014). WAY and ESP are both dominated by Cunoniaceae, Clusiaceae, Rosaceae, Melastomataceae (ESP) and Lauraceae (WAY). The species composition of these plots leads us to describe ESP (dominated by *Weinmannia bangii* Rusby, Cunoniaceae) as an older forest stand than WAY (dominated by *Weinmannia crassifolia* Ruiz & Pav. and the presence of successional species from the genera *Pentacalia*, Asteraceae, *Ageratina*, Asteraceae, and *Hesperomeles*, Rosaceae). The high *NPP* reported in

the present study and the low basal area, low incidence of large trees, high density of small dbh-size class stems, and high recruitment rates reported by W. Farfan Rios et al. (unpublished data) in the WAY plot lead us to speculate that this forest could be recovering from past disturbance.

Overall, the total stand biomass, *NPP* and *GPP*, in this site are lower than that reported from lowland or lower montane forests located below the cloud immersion zone (Table 2). However, the NPP_{total} reported here is higher than our previous estimates from WAY (5.09 ± 0.42 Mg C ha^{-1} year^{-1}, Girardin et al. 2010), a difference driven by NPP_{canopy} (which now includes herbivory), $NPP_{ACW < 10cm}$ (now directly measured), $NPP_{branch turnover}$ (now directly measured) and $NPP_{fine roots}$ (now corrected for underestimation during sampling). The R_h and R_a values reported here also take precedence over our previous estimates, as they are directly measured from a partitioning experiment. A more complete intensive measurement regime and a different measurement period (inter-annual variability) may explain an increase in *NPP* (and hence *GPP*) estimates between studies, hence the values reported here take precedence over our previously reported estimates (Girardin et al. 2010; Malhi et al. 2014). The present analysis also suggests a discrepancy between detailed ground measurements and the theory behind *GPP* modelling. Our estimate of *GPP* was significantly higher than a previous estimate from a simulated annual *GPP* (2008–2009), using the Soil Plant Atmosphere (SPA) canopy model with detailed full canopy physiology data (16.2 ± 1.6 Mg C ha^{-1} year^{-1}, van de Weg et al. 2012). The SPA model is well-validated and has a good track record from other tropical forests. In this study, we have high confidence in our estimates of *NPP*. However, our values of R_a may be overestimated due to scaling R_{stem} from surface area data. This study estimated an R_{stem} fraction of 35/45% of R_a, exceeding the typical fraction of 23.5% suggested by Malhi et al. (2009). In both plots, our estimates of R_a were significantly higher than those of an Alpine temperate forest treeline ecosystem (12.4 Mg C ha^{-1} year^{-1}, Wieser 2007).

Many landscape-scale carbon cycling models assume a constant *CUE* value of 0.5 (DeLucia et al. 2007). Despite the significantly higher *NPP* and *GPP* values reported in WAY, both forests maintained a *CUE* ($0.32 \pm 0.04/0.30 \pm 0.04$) typical of tropical old growth forests, ca. 0.3 to ca. 0.5 (Chambers et al. 2000; Giardina et al. 2003; Litton et al. 2007; Malhi et al. 2014). However, stem *CUE* ($NPP_{ACW}/NPP_{ACW} + R_{stem}$) was higher in ESP ($0.24 \pm 0.39$) than WAY ($0.15 \pm 0.22$). Root *CUE* did not differ significantly between plots ($0.31 \pm 0.92/0.33 \pm 0.92$).

Despite the difference in total *NPP* between the two plots, the pattern of allocation of *NPP* to canopy (42%/50%), wood (38%/26%) and roots (20%/24%) was relatively similar for the two sites, although a higher proportion of *NPP* was allocated to the canopy and to above-ground coarse wood in WAY (Table 6). For a given *NPP* component, a similar fraction of *NPP* was allocated in both plots although *NPP* was substantially lower in ESP. In a

Table 6. Carbon allocation to above- and below-ground components of *NPP* and partitioning of respiration components in Esperanza and Wayqecha, Peru, 2009–2010.

Total carbon allocation	Esperanza mean (±SE)	Wayqecha mean (±SE)
Above-ground carbon (Mg C ha^{-1} year^{-1})	16.72 (±0.86)	19.43 (±0.99)
Below-ground carbon (Mg C ha^{-1} year^{-1})	5.56 (±0.33)	7.36 (±0.54)
Above-ground fraction	0.75 (±0.04)	0.73 (±0.04)
Below-ground fraction	0.25 (±0.01)	0.27 (±0.02)
Allocation of *NPP*		
Canopy	0.42 (±0.07)	0.50 (±0.06)
Above-ground coarse wood	0.38 (±0.02)	0.26 (±0.02)
Fine roots	0.20 (±0.03)	0.24 (±0.04)
Partitioning of autotrophic respiration		
Canopy	0.40 (±0.04)	0.28 (±0.03)
Wood	0.42 (±0.04)	0.54 (±0.04)
Rhizosphere	0.18 (±0.02)	0.18 (±0.02)

All values other than above- and below-ground carbon are fractions. SE, standard error of the mean.

recent review of *NPP* allocation at 35 tropical forest sites including WAY and several other cloud montane forest sites along the Kosñipata elevation transect, Malhi et al. (2011) reported that tropical forests typically partitioned allocation equally between the three main components (34 ± 6% to canopy, 39 ± 10% to wood and 27 ± 11% to fine roots), and that *NPP* allocated to the canopy ranged from ca. 25% to 45% across sites. In the montane cloud forest sites of Kosñipata, the allocation of *NPP* to canopy components was at the higher end of the range; this may partially be explained by our inclusion of herbivory to *NPP*$_{canopy}$, a term that had not been measured before.

Finally, this comprehensive 'bottom-up' approach to estimating the forest carbon budget provided an opportunity to cross-check our results, ensuring the robustness of our findings. We were able to determine how much we might have underestimated *NPP* by comparing total net primary productivity (*NPP*$_{total}$) with measured heterotrophic respiration (*R*$_h$, root free soil and coarse woody debris). For a forest ecosystem close to equilibrium, heterotrophic respiration should equal *NPP*. Hence, the difference between our measured *R*$_h$ and our predicted *R*$_h$ (estimated as *NPP*$_{total}$) provides an indication of the robustness of our estimates. For estimates of coarse woody debris respiration (to be added to soil heterotrophic respiration), we used values from Gurdak et al. (2012) from WAY. We estimated the difference between *R*$_h$ and *NPP* to be 1.26 ± 0.59 Mg C ha^{-1} year^{-1} (*R*$_h$ is larger), not significantly different from zero. This increases our confidence that our measurements of *NPP* were close to comprehensive. We estimate the ratio r = (*NPP* − *R*$_h$)/*R*$_h$ to be –0.13 ± 0.25, not significantly different from zero. A value of r neighbouring zero indicates that our estimates are nearly closing the heterotrophic cycle of the ecosystem. A negative value of r suggests that there is a net carbon source in the soil and necromass, as it is unlikely that we underestimated *NPP*.

Conclusions

This study presents the first comprehensive description of the carbon cycle and seasonal variation in the carbon budget

for an upper montane cloud forest located near the tree-line. Most remarkably, we have been able to describe the seasonal variation in the components of *NPP*, autotrophic respiration, *GPP* and *CUE* for the first time. We found close linkages between the seasonal trends in climate variables (in particular solar radiation, driven by cloud immersion frequency) and the seasonal budget of *NPP* components. Nonetheless, we suggest that seasonality trends of litterfall are driven by phenological rhythms of dominant tree families rather than being directly driven by the cloud immersion regime.

We report stronger seasonality in the components of *NPP* than that found for *R*$_a$, with an increase in *CUE* led by higher *NPP* during the wet season. Our findings suggest that trees invest more in the basic function of biomass productivity in the cooler, darker season and more in maintenance and reproduction during the dry season.

We report slight differences in carbon cycling (most notably in *GPP*) between the two plots, despite their similarities in climate and soil conditions. We suggest that these may be explained by different stand ages and species composition, rather than solely by microclimate variations. The study shows that there are differences in carbon dynamics compared to lowland and lower montane sites (lower *NPP* and *GPP*), as well as surprising similarities (e.g. *CUE*).

Overall, the paper demonstrates the power of a detailed comprehensive approach to estimating each component of the forest carbon cycle, and presents its first application to a tropical montane forest system. Such approaches can greatly increase our understanding of the dynamics of the carbon cycle and its relationship with climate.

Notes on contributors

Cécile A.J. Girardin is an ecosystems scientist who focuses on carbon dynamics of tropical forest ecosystems. She coordinates the Global Ecosystems Monitoring Network.

Javier E. Silva-Espejo, Luiz Aragao, William Farfan, Karina García Cabrera, Darcy F. Galiano-Cabrera, Lidia P. Huaraca-Quispe, Ivonne Alzamora-Taype, Luzmila Eguiluz-Mora, Liliana Durand-Baca, Joshua B. Fisher, Norma Salinas, Daniel B. Metcalfe Miles Silman and Patrick Meir are tropical forest ecologists who all contributed by establishing the study areas, contributing data and advice on the interpretation of results.

Christopher E. Doughty is a junior research fellow. His main interest is understanding tropical forest carbon fluxes, through remote sensing, eddy covariance, leaf gas exchange and intensive carbon cycle plots.

Toby R. Marthews is a postdoctoral researcher. Dr Marthews's research is on forest and woodland ecosystem dynamics both through simulation work and fieldwork.

Katherine Halladay has worked on clouds and climate in the Andean transect.

Yadvinder Malhi, Senior Research Fellow and director of the Oxford Centre for Tropical Forests, leads the Ecosystems Programme of the Environmental Change Institute, with a focus of understanding the functioning of tropical forests and their response to global change.

References

Aragão LEOC, Malhi Y, Metcalfe DB, Silva-Espejo JE, Jimenez E, Navarrete D, Almeida S, Costa ALC, Salinas N, Phillips OL, et al. 2009. Above- and below-ground net primary productivity across ten Amazonian forests on contrasting soils. Biogeosciences 6:2759–2778.

Aragão LEOC, Malhi Y, Roman-Cuesta RM, Saatchi S, Anderson LO, Shimabukuro YE. 2007. Spatial patterns and fire response of recent Amazonian droughts. Geophysical Research Letters 34(7). doi:10.1029/2006GL028946.

Araújo AC, Nobre AD, Kruijt B, Elbers JA, Dallarosa R, Stefani P, von Randow C, Manzi AO, Culf AD, Gash JHC, et al. 2002. Comparative measurements of carbon dioxide fluxes from two nearby towers in a central Amazonian rainforest: The Manaus LBA site. Journal Geophysical Research 107(D20):8090.

Atkin OK, Evans JR, Ball MC, Lambers H, Pons TL. 2000. Leaf respiration of snow gum in the light and dark. interactions between temperature and irradiance. Plant Physiology 122:915–923.

Bruijnzeel LA, Veneklaas E. 1998. Climatic conditions and tropical montane forest productivity: the fog has not lifted yet. Ecology 78:3–9.

Bruijnzeel LA, Waterloo JM, Proctor J, Kuiters AT, Kotterink B. 1993. Hydrological observations in montane rain forests on Gunung Silam, Sabah, Malaysia, with special reference to the "Massenerhebungeffect". Journal of Ecology 81:145–167.

Bubb P, May I, Miles L, Sayer J. 2004. Cloud forest agenda. Cambridge (UK): UNEP-WCMC.

Cairns MA, Brown S, Helmer EH, Baumgardner GA. 1997. Root biomass allocation in the world's upland forests. Oecologia 111:1–11.

Chambers JQ, dos Santos J, Ribeiro RJ, Higuchi N. 2001. Tree damage, allometric relationships, and above-ground net primary production in central Amazon forest. Forest Ecology and Management 152:73–84.

Chambers JQ, Higuchi N, Schimel JP, Ferreira LV, Melack JM. 2000. Decomposition and carbon cycling of dead trees in tropical forests of the central Amazon. Oecologia 122:219–223.

Chambers JQ, Tribuzy ES, Toledo LC, Crispim BF, Higuchi N, dos Santos J, Araujo AC, Kruijt B, Nobre AD, Trumbore SE. 2004. Respiration from a tropical forest ecosystem: partitioning of sources and low carbon use efficiency. Ecological Applications 14:S72–S88.

Chave J, Andalo C, Brown S, Cairns MA, Chambers JQ, Eamus D, Folster H, Fromard F, Higuchi N, Kira T, et al. 2005. Tree allometry and improved estimation of carbon stocks and balance in tropical forests. Oecologia 145:87–99.

Chave J, Navarrete D, Almeida S, Alvarez E, Aragao LEOC, Bonal D, Chatelet P, Silva-Espejo JE, Goret JY, von Hildebrand P, et al. 2010. Regional and seasonal patterns of litterfall in tropical South America. Biogeosciences 7:43–55.

Churchill SP, Balsley H, Forero E, Luteyn J, editors. 1996. Biodiversity and conservation of Neotropical Montane forests. New York: New York Botanical Garden.

Clark DA, Brown S, Kicklighter DW, Chambers JQ, Thomlinson JR, Ni J, Holland EA. 2001. Net primary production in tropical forests: an evaluation and synthesis of existing field data. Ecological Applications 11:371–384.

Colwell RK, Brehm G, Cardelús CL, Gilman AC, Longino JT. 2008. Global warming, elevational range shifts, and lowland biotic attrition in the wet Tropics. Science 322(5899): 258–261.

DeLucia EH, Drake JE, Thomas RB, Gonzalez-Meler M. 2007. Forest carbon use efficiency: is respiration a constant fraction of gross primary production? Global Change Biology 13:1157–1167.

Demareza V, Duthoita S, Baretb F, Weissb M, Dedieu G. 2008. Estimation of leaf area and clumping indexes of crops with hemispherical photographs. Agricultural and Forest Meteorology 148:644–655.

Doughty CE, Goulden ML. 2008. Seasonal patterns of tropical forest leaf area index and CO_2 exchange. Journal of Geophysical Research–Biogeosciences 113(G1):1–12.

Feeley KJ, Silman MR. 2010. Land-use and climate change effects on population size and extinction risk of Andean plants. Global Change Biology 16:3215–3222.

Feldpausch TR, Banin L, Phillips OL Baker TR, Lewis SL, Quesada CA, Affum-Baffoe K, Arets EJMM, Berry NJ, Bird M, et al. 2011. Height-diameter allometry of tropical forest trees. Biogeosciences 8(5):1081–1106.

Foster P. 2001. The potential negative impacts of global climate change on tropical montane cloud forests. Earth-Science Reviews 55:73–106.

Gentry AH, Ortiz SR. 1993. Patrones de composición floristica en la Amazonia Peruana. In: Kalliola R, Puhakkaa M, Danjoy W, editors. Amazonia Peruana - vegetación húmeda tropical en el llano subandino. Turku (Finland): Turku University Press. p. 155–166.

Giardina CP, Ryan MG, Binkley D, Fownes JH. 2003. Primary production and carbon allocation in relation to nutrient supply in a tropical experimental forest. Global Change Biology 9:1438–1450.

Girardin CAJ, Aragao L, Malhi Y, Huaraca Huasco W, Metcalfe D, Durand L, Mamani M, Silva-Espejo JE, Whittaker RJ. 2013. Fine root dynamics along an elevational gradient in tropical Amazonian and Andean forests. Global Biogeochemical Cycles 27:252–264.

Girardin CAJ, Farfan W, Garcia K, Feeley K, Jørgensen PM, Killeen T, Malhi Y, Araujo Murakami A, Cayola Pérez L, Renate S, et al. 2014. Spatial patterns of above-ground

structure, biomass and composition ina network of six Andean elevation transects. Plant Ecology & Diversity 7(1–2): 161–171.

Girardin CAJ, Malhi Y, Aragão LEOC, Mamani-Solórzano M, Huaraca Huasco W, Durand L, Feeley KJ, Rapp J, Silva-Espejo JE, Silman MR, et al. 2010. Net primary productivity allocation and cycling of carbon along a tropical forest elevational transect in the Peruvian Andes. Global Change Biology 16:3176–3192.

Graefe S, Hertel D, Leuschner C. 2008. Fine root dynamics along a 2000 m elevation transect in South Ecuadorian mountain rainforests. Plant and Soil 313:155–166.

Grubb PJ. 1977. Control of forest growth and distribution on wet tropical mountains: with special reference to mineral nutrition. Annual Review of Ecology and Systematics 8: 83–107.

Gurdak D, Rozas-Dávila A, Aragão LEOC, Huaraca Huasco W, Doughty C, Metcalfe DB, Farfan Rios W, García Cabrera K, Silva Espejo JE, Silman MRR, et al. In press, 2012. Balancing above ground carbon fluxes and wood debris respiration to understand dynamics of biomass along a tropical Andes to Amazon elevational gradient.

Harmon ME, Whigham DF, Sexton J, Olmsted I. 1995. Decomposition and mass of woody detritus in the dry tropical forests of the Northeastern Yucatan Peninsula, Mexico. Biotropica 27:305–316.

Heinemeyer A, Hartley IP, Evans SP, Carreira de la Fuente JA, Ineson P. 2007. Forest soil CO_2 flux: uncovering the contribution and environmental responses of ectomycorrhizas. Global Change Biology 13:1786–1797.

Herbert DA, Fownes JH. 1999. Forest productivity and efficiency of resource use across a chronosequence of tropical montane soils. Ecosystems 2:242–254.

Hughes IG, Hase TPA. 2010. Measurements and their uncertainties: a practical guide to modern error analysis.Oxford (UK): Oxford University Press.

Jackson RB, Canadell J, Ehleringer JR, Mooney HA, Sala OE, Schulze ED. 1996. A global analysis of root distributions for terrestrial biomes. Oecologia 108:389–411.

Kappelle M, Brown AD. 2001. Bosques nublados del neotropico. Heredia, CR. Costa Rica: Instituto Nacional de Biodiversidad, INBio.

Killeen T, Douglas M, Consiglio T, Jørgensen P, Mejia J. 2007. Dry spots and wet spots in the Andean hotspot. Journal of Biogeography 34:1357–1373.

Kitayama K, Aiba SI. 2002. Ecosystem structure and productivity of tropical rain forests along altitudinal gradients with contrasting soil phosphorus pools on Mount Kinabalu, Borneo. Journal of Ecology 90:37–51.

Körner C. 2012. Water, nutrient and carbon relations, In: Alpine treelines. Functional ecology of the global high elevation tree limits. Basel (Switzerland): Springer. ISBN 978-3-0348-0396-0.

Leigh EG. 1999. Tropical forest ecology: a view from Barro Colorado Island. New York (NY): Oxford University Press.

Leuschner C, Moser G, Bertsch C, Röderstein M, Hertel D. 2007. Large altitudinal increase in tree root/shoot ratio in tropical mountain forests of Ecuador. Basic and Applied Ecology 8:219–230.

Lewis SL, Lloyd J, Sitch S, Mitchard ETA, Laurance WF. 2009. Changing ecology of tropical forests: evidence and drivers. Annual Review of Ecology, Evolution and Systematics 40:529–549.

Litton CM, Raich JW and Ryan MG. 2007. Carbon allocation in forest ecosystems. Global Change Biology 13:2089–2109.

Lloyd J, Patiño S, Paiva RQ, Nardoto GB, Quesada CA, Santos AJB, Baker TR, Brand WA, Hilke I, Gielmann H, et al. 2010. Optimisation of photosynthetic carbon gain and within-canopy gradients of associated foliar traits for Amazon forest trees. Biogeosciences 7:1833–1859.

Lowman MD. 1984. An assessment of techniques for measuring herbivory: is rain forest defoliation more intense than we thought? Biotropica 16:264–68.

Lowman MD. 1985. Temporal and spatial variability in insect grazing of the canopies of five Australian rain forest tree species. Australian Journal of Ecology 10:7–24.

Luyssaert S, Inglima I, Jung M, Richardson AD, Reichstein M, Papale D, Piao SL, Schulze ED, Wingate L, Matteucci G, et al. 2007. CO_2 balance of boreal, temperate, and tropical forests derived from a global database. Global Change Biology 13:2509–2537.

Malhi Y, Aragao LEOC, Metcalfe DB, Paiva R, Quesada CA, Almeida S, Anderson L, Brando P, Chambers JQ, da Costa ACL, et al. 2009. Comprehensive assessment of carbon productivity, allocation and storage in three Amazonian forests. Global Change Biology 15:1255–1274.

Malhi Y, Baker TR, Phillips OL, Almeida S, Alvarez E, Arroyo L, Chave J, Czimczik CI, Di Fiore A, Higuchi N, et al. 2004. The above-ground coarse wood productivity of 104 neotropical forest plots. Global Change Biology 10:563–591.

Malhi Y, Doughty C, Galbraith D. 2011. The Allocation of Ecosystem Net Primary Productivity in Tropical Forests. Philosophical Transactions of the Royal Society 366 (1582):3225–3245 .

Malhi Y, Farfán Amézquita F, Doughty CE, Silva-Espejo JE, Metcalfe DB, Aragão LEOC, Girardin CAJ, Huaraca-Quispe LP, Alzamora-Taype I, et al. 2014. The productivity, metabolism and carbon cycle of two lowland tropical forest plots in south-western Amazonia, Peru. Plant Ecology & Diversity 7(1–2):85–105.

Malhi Y, Nobre AD, Grace J, Kruijt B, Pereira MGP, Culf A, Scott S. 1998. Carbon dioxide transfer over a Central Amazonian rain forest. Journal of Geophysical Research-Atmospheres 103:31593–31612.

Malhi Y, Phillips OL, Lloyd J, Baker TR, Wright J, Almeida S, Arroyo L, Frederiksen T, Grace J, Higuchi N, et al. 2002. An international network to monitor the structure, composition and dynamics of Amazonian forests (RAINFOR). Journal of Vegetation Science 13:439–450.

Malhi Y, Silman M, Salinas N, Bush M, Meir P, Saatchi S. 2010 Introduction: elevation gradients in the tropics: laboratories for ecosystem ecology and global change research. Global Change Biology 16:3171–3175.

Malhi Y, Wood D, Baker TR, Wright J, Phillips OL, Cochrane T, Meir P, Chave J, Almeida S, Arroyo L, et al. 2006. The regional variation of aboveground live biomass in old-growth Amazonian forests. Global Change Biology 12:1107–1138.

Malhi Y, Wright J. 2004. Spatial patterns and recent trends in the climate of tropical rainforest regions. Philosophical Transactions of the Royal Society of London B 359:311–329.

Marthews TR, Malhi Y, Girardin CAJ, Silva-Espejo JE, Aragão LEOC, Metcalfe DB, Rapp JM, Mercado LM, Fisher RA, Galbraith DR, et al. 2012a. Simulating forest productivity along a neotropical elevational transect: temperature variation and carbon use efficiency. Global Change Biology 18:2882–2898.

Marthews TR, Metcalfe D, Malhi Y, Phillips O, Huaraca Huasco W, Riutta T, Ruiz Jaén M, Girardin CAJ, Urrutia R, Butt N, et al. 2012b. Measuring tropical forest carbon allocation and cycling: a RAINFOR-GEM field manual for intensive census plots (v2.2). Manual. Global Ecosystems Monitoring Network. Available from http://gem.tropicalforests.ox.ac.uk/.

Martin AR, Thomas SC. 2011. A reassessment of carbon content in tropical trees. PlosOne 6:e23533.

Meir P, Grace J, Miranda AC. 2001. Leaf respiration in two tropical rain forests: constraints on physiology by phosphorus, nitrogen and temperature. Functional Ecology 15: 378–387.

Metcalfe DJ, Grubb PJ. 1997. The responses to shade of seedlings of very small-seeded tree and shrub species from tropical rain forest in Singapore. Functional Ecology 11:215–221.

Metcalfe DB, Meir P, Aragao LEOC, Lobo-do-Vale R, Galbraith D, Fisher RA, Chaves MM, Maroco JP, da Costa ACL, de Almeida SS, et al. 2010. Shifts in plant respiration and carbon use efficiency at a large-scale drought experiment in the eastern Amazon. New Phytologist 187:608–621.

Metcalfe DB, Meir P, Aragao LEOC, Malhi Y, da Costa ACL, Braga A, Goncalves PHL, de Athaydes J, de Almeida SS, Williams M. 2007. Factors controlling spatio-temporal variation in carbon dioxide efflux from surface litter, roots, and soil organic matter at four rain forest sites in the eastern Amazon. Journal of Geophysical Research–Biogeosciences 112: G04001. doi:10.1029/2007JG000443.

Miller SD, Goulden ML, da Rocha HR. 2007. The effect of canopy gaps on subcanopy ventilation and scalar fluxes in a tropical forest. Agricultural and Forest Meteorology 142(1):25–34.

Moser G, Röderstein M, Soethe N, Hertel D, Leuschner C. 2008. Altitudinal changes in stand structure and biomass allocation of tropical mountain forests in relation to microclimate and soil chemistry. In: Beck E, Bendix J, Kottke I, Makeschin F, Mosandl R, editors. Gradients in a tropical mountain ecosystem of Ecuador. Ecological Studies. Vol. 198. Berlin (Germany): Springer Verlag. p. 229–242.

Myers N, Mittermeier RA, Mittermeier CG, da Fonseca GAB, Kent J. 2000. Biodiversity hotspots for conservation priorities. Nature 403:853–858.

Phillips OL, Baker TR, Arroyo L, Higuchi N, Killeen TJ, Laurance WF, Lewis SL, Lloyd J, Malhi Y, Monteagudo A, et al. 2004. Pattern and process in Amazon tree turnover, 1976–2001. Philosophical Transactions of the Royal Society B 359:381–407.

Pounds JA, Fogden MPL, Campbell JH. 1999. Biological response to climate change on a tropical mountain. Nature 398:611–615.

Raich, JW. 1997. Above-ground productivity and soil respiration in three Hawaiian rain forests. Forest Ecology and Management 107:309–318.

Raich JW. 1997. Above-ground productivity and soil respiration in three Hawaiian rain forests. Forest Ecology and Management 107:309–318.

Rapp JM, Silman MR. Forthcoming 2013. Diurnal, seasonal, and altitudinal trends in microclimate across a 3900 meter altitudinal gradient in the humid tropics. Climate Research.

Reich PB, Ellsworth DS, Walters MB. 1998. Leaf structure (specific leaf area) modulates photosynthesis-nitrogen relations: evidence from within and across species and functional groups. Functional Ecology 12:948–958.

Robertson AL, Malhi Y, Farfan F, Aragão LEOC, Silva EJ, Roberson MA. 2010. Stem respiration in tropical forests along an elevation gradient in the Amazon and Andes. Global Change Biology 16:3193–3204.

Röderstein M, Hertel D, Leuschner C. 2005. Above- and belowground litter production in three tropical montane forests in southern Ecuador. Journal of Tropical Ecology 21:483–492.

Schuur EAG, Matson PA. 2001. Net primary productivity and nutrient cycling across a mesic to wet precipitation gradient in Hawaiian montane forest. Oecologia 128:431–442.

Still CJ, Foster PN, Schneider SH. 1999. Simulating the effects of climate change on tropical montane cloud forests. Nature 398:608–610.

Tanner EVJ, Grubb PJ. 1999. 1974–1978 dataset. *NPP* tropical forest: John Crow ridge, Jamaica. Oak Ridge (TN): Oak Ridge National Laboratory Distributed Active Archive Centre.

Tanner EVJ, Vitousek PM, Cuevas E. 1998. Experimental investigation of nutrient limitation of forest growth on wet tropical mountains. Ecology 79:10–22.

Torres C, Galetto L. 2011. Flowering phenology of co-occurring Asteraceae: a matter of climate, ecological interactions, plant attributes or of evolutionary relationships among species? Organisms Diversity and Evolution 11:9–19.

van de Weg MJ, Meir P, Grace J, Ramos GD. 2012. Photosynthetic parameters, dark respiration and leaf traits in the canopy of a Peruvian tropical montane cloud forest. Oecologia 168:23–34.

van Oijen M, Schapendonk A, Höglind M. 2010. On the relative magnitudes of photosynthesis, respiration, growth and carbon storage in vegetation. Annals of Botany 105:793–797.

van Schaik C, Terborgh J, Wright S. 1993. The phenology of tropical forests: adaptive significance and consequences for primary consumers. Annual Review of Ecology and Systematics 24:353–377.

Vitousek PM, Sanford RL. 1986. Nutrient cycling in moist tropical forest. Annual Review of Ecology and Systematics 17:137–16.

Vogt KA, Vogt DJ, Bloomfield J. 1998. Analysis of some direct and indirect methods for estimating root biomass and production of forests at an ecosystem level. Plant Soil 200:71–89.

Waide RB, Zimmerman JK, Scatena FN. 1998. Controls of primary productivity: lessons from the Luquillo mountains in Puerto Rico. Ecology 79:31–37.

Wieser G. 2007. Limitation by an insufficient carbon assimilation and allocation. In: Wieser G, Tausz M, editors. Trees at their upper limit. Dordrecht (The Netherlands): Springer. p. 79–129.

Young KR.1992. Biogeography of the montane forests zone of the Eastern slopes of Peru. Memorias del Museo de Historia Natural, 21. Biogeografía, Ecología y Conservación del bosque Montano en el Perú. Peru: Universidad Nacional Mayor de San Marcos. p. 119–141.

Zanne AE, Lopez-Gonzalez G, Coomes DA, Ilic J, Jansen S, Lewis SL, Miller RB, Swenson NG, Wiemann MC, Chave J. 2009. Towards a worldwide wood economics spectrum [Internet]. Dryad Digital Repository. doi: 10.5061/dryad.234.

Zimmerman JK, Wright S, Calderon O, Aponte Pagan M, Paton S. 2007. Flowering and fruiting phenologies of seasonal and aseasonal neotropical forests: the role of annual changes in irradiance. Journal of Tropical Ecology 23:231–251.

Zimmermann M. 2009. Diurnal variation in soil respiration in a montane cloud forest in Peru. Soil Biology and Biochemistry 41:1338–1340.

Zimmermann M. 2010. Temporal variation and climate dependence of soil respiration and its components along a 3000 m altitudinal tropical forest gradient. Global Biogeochemical Cycles 24:GB4012. doi:10.1029/2010GB003787.

Zimmermann M, Meir P, Bird MI, Malhi Y, Ccahuana AJQ. 2009. Climate dependence of heterotrophic soil respiration from a soil-translocation experiment along a 3000 m tropical forest altitudinal gradient. European Journal of Soil Science 60:895–906.